NRIAG JOURNAL OF ASTRONOMY AND GEOPHYSICS
2022, VOL. 11, NO. 1, 224–236
https://doi.org/10.1080/20909977.2022.2067680

Reservoir characterisations from bouguer gravity data, Northern Western Desert, Egypt

Haby S. Mohamed, Mahmoud M. Senosy and Mahmoud Talat

Geology Department, Faculty of Science, Assiut University, Assiut Egypt

ABSTRACT

The current study is a trial for estimating the reservoir characterizations as density, effective porosity, and hydrocarbon saturation. It employs subsurface lithological data from 48 drilled wells dispersed over the area and gravity data. The study was based on applying the gravity stripping technique. The gravities of five well-defined depositional cycles (cycle I, II, III, IV, V) of diverse ages were calculated depending on each cycle's density and thickness obtained from the available well data. Maps were prepared for each cycle and the surface of basement rocks from which the characteristic structures were traced. New linear empirical relationships were concluded with a correlation coefficient of 0.9 from linear relationships. Accordingly, reservoir characterizations were calculated for the reservoir at the sites in which neither seismic nor well logging data are available. Contour maps were prepared for each parameter to reveal the areal distribution of these parameters in all study areas. Maps revealed that, at Abu Gharadig basin, the predicted density varies from 2.3 g/cm3 to 2.7 g/cm3, effective porosity from 13% to 30%, and hydrocarbon saturation from 50% to 90%. The main deep subsurface structure trends are the E-W, the WNW-ESE, the ENE-WSW, the NE-SW, the NW-SE, and the N-S trends.

ARTICLE HISTORY
Received 23 February 2022
Revised 4 April 2022
Accepted 14 April 2022

KEYWORDS
Abu Gharadig basin; bouguer gravity; stripping technique; reservoir characterisation

1. Introduction

Egypt's Northern Western Desert is considered one of the most important oil-producing regions, as it contains many significant and potential basins and has a dynamic depositional history (particularly the Abu Ghradig Basin). The Abu Gharadig basin has a large portion of the subsurface sediments, which are considered reservoir rocks where the members of the Lower Cenomanian, Albian and Upper Cenomanian to Maastrichtian. The potential source rocks are found in the Abu Roash "F" member and Khatatba Formation (El-Shaarawy et al. 1994). Therefore, it has attracted the attention of many researchers and companies to study hydrocarbon potentiality using seismic data and well logs.

Latitudes 28° 20´N and 30°10´N and longitudes 26° 30´E and 31°E represent the location of the study area, including the Abu Ghradig basin (Figure 1a). The Kattaniya horst to the east and the Qattara Depression to the west is the Abu Gharadig basin. To the north and south, it is limited by two basement uplifts; the northern uplift is coupled with the Sharib-Rabat platform, while the southern uplift is correlated with the Cairo-Bahariya uplift (Meshref et al. 1980).

Several authors have investigated Upper Cretaceous reservoir characterisations of the Abu Roash "G" Member, Baharyia Formation in the research area. El-Hossainy (2008) considered the Bahariya Formation in the Abu Gharadig field an excellent grade reservoir, noting that permeability improves as one moves northeast. The petrophysical features of the Bahariya Formation in the Aghar oil field and Meleiha-NE oil field, according to Gadallah et al. (2004) (Gadallah et al. 2010), provide information regarding the formation's potential to store and produce oil. According to Abu Shady et al. (2010), the Upper Bahariya reservoir was primarily composed of sandstone (with a bulk density of 2.2 to 2.65 g/cm^3), indicating a mix of clay and lime cement. According to Bekhiet et al. (2011), the effective porosity of the Abu Roash "G" Member ranges from 18.3% to 21.2%, whereas the water saturation ranges from 15.1% to 92.3%. The geostatic model for evaluating the 3-D geometry of the Abu Roash G Formation in the Amana field east of Abu Gharadig basin was built by Abu-Hashish and Said (2016), where the source rock is the Upper Jurassic Khatatba Formation. He concluded that the porosity ranged from 19% to 22%, water saturation was 18–40%, and the average permeability was 40 md. There is a positive relationship between porosity and permeability from the petrographical and petrophysical investigation of the Upper Bahariya sandstone in the SW Sennan field (Abuseda et al. 2016). Based on the petrophysical analysis of the Bahariya formation in BED-1 and BED-4 oil fields of the North-Western Desert,

CONTACT Haby S. Mohamed habysalaheldin@yahoo.com Geology Department, Faculty of Science, Assiut University, Assiut 71516, Egypt

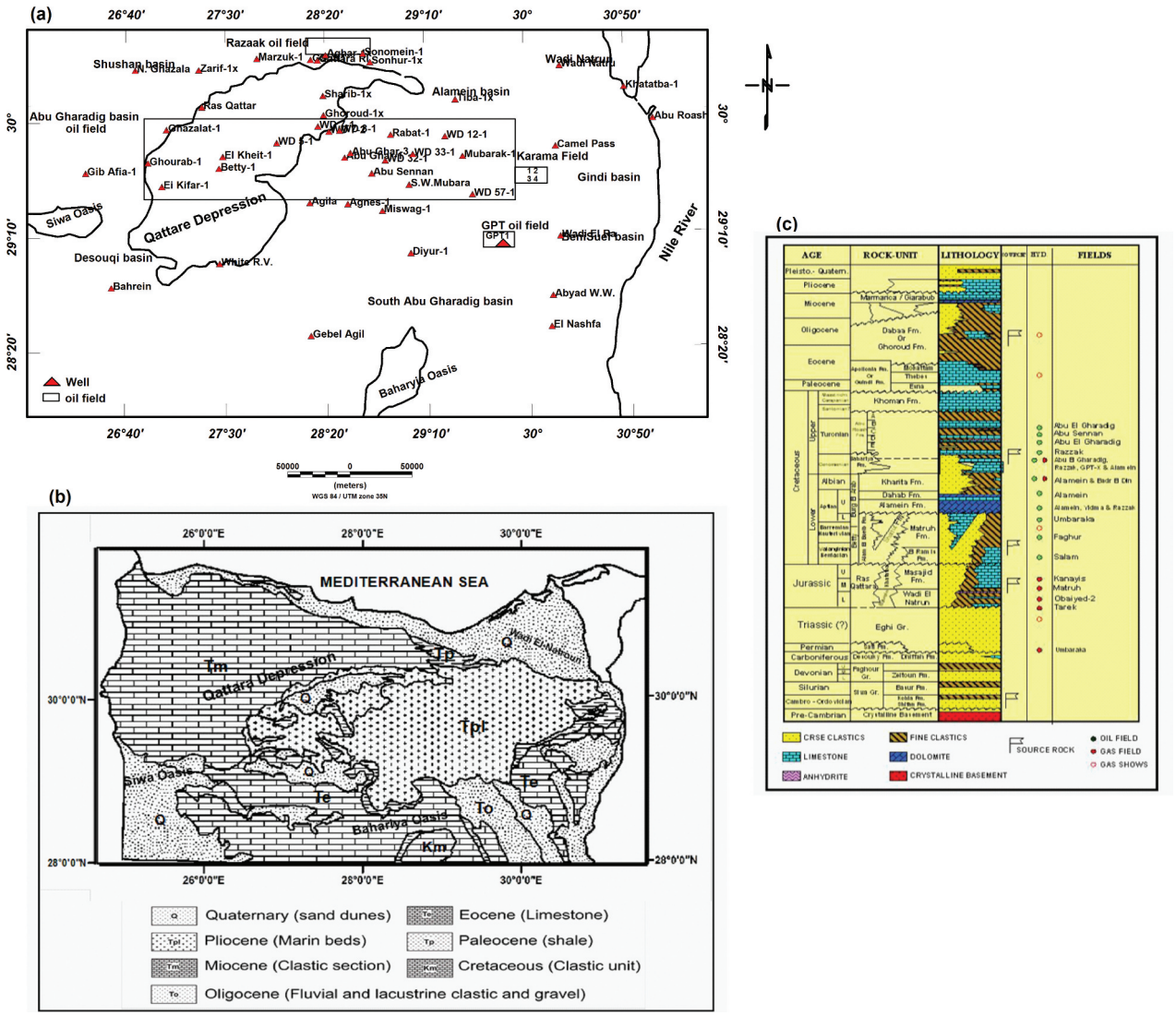

Figure 1. A) Location map of the study area, including deep wells; b) North Western Desert geological map (adapted from Egypt's geological map, 1981); and c) North Western Desert generalised litho-stratigraphic column (Schlumberger 1995).

Mohamed et al. (2016a) concluded that the Bahariya Formation consists mainly of sandstone with interbedded shale and siltstone. The oil shale content is increasing in the northwest and southeast direction. The Upper Bahariya Formation of the Tut oil field has an effective porosity range from 13% to19% and shale volume from 19% to35% (Aboelhassan et al. 2017). El-Bagoury (2019, 2020) integrated core analysis and well logs to study water saturation properties in Bahariya shaley sand reservoirs of Neag-1, −2, and −3. The upper part of the Bahariya reservoir is different in clay contents and porosity due to fining and coarsening upward. Saleh et al. (2021) evaluated the characterisation of the Abu Roash (G) reservoir in the Karama oil field using well logs and petrophysical core data, and the results suggested a promising reservoir. He concluded that effective porosity ranged from 18.3% to 33.3%, with hydrocarbon saturation exceeding 61.5% in some zones.

Seismic and log data are generally used for reservoir characterisation. In addition to being costly and difficult to obtain, data are not available in all areas. The study area is one area that is not fully covered by well logs or seismic profiles. A new experiment was conducted that utilises Bouguer gravity data to estimate the characteristics (density, hydrocarbon saturation, and porosity) of the Upper Cretaceous reservoir to address this matter. Gravity survey and its wide coverage ability area represent a low cost compared to acquiring seismic and log data. Such an experiment will provide a preliminary assessment of the expected reservoirs that will be considered a guide to comprehensive seismic surveying and exploration of wells.

2. Geologic and structure setting

The distribution of sediments in the Western Desert follows a simple north–south trend: sand percentage and degree rise from shallow marine to primarily continental to the south, while carbonate rocks are more frequent in the north, except stratigraphic intervals that correlate to the transgression towards the south as noted by (Sestini 1995) (Figure 1b). The study area is on an unstable continental shelf with a thick stratigraphic column from the Pre-Cambrian basement complex to Recent (Keeley 1989). This stratigraphic column comprises five sedimentation cycles of clastics to carbonates sediments as defined by EGPC (1992) (Figure 1c). These cycles have been arranged from old to recent as follows:

- Clastic facies Cycle I includes the oldest sedimentary strata (the entire Palaeozoic and Lower Jurassic formations).
- The carbonate section of Middle and Upper Jurassic formations, which comprises the Khatatba, Wadi El Natrun, and Masajid formations, is known as Cycle II facies.
- Cycle III of clastic facies spans the Lower Cretaceous to the Upper Cretaceous Early Cenomanian (Alam El Bueib, Kharita, Bahariya, Abu Roash G, and Khoman formations).
- Cycle IV comprises the Abu Roash A, B, C, D, E, F, Khoman, Mokattam, and Gindi formations, spanning the Upper Cenomanian to the Middle Eocene.
- Cycle V: It comprises Upper Eocene, Oligocene, Miocene, and newer clastic facies (Dabaa and Kurkur formations).

The major hydrocarbon resources in the Western Desert are found in Upper Cretaceous sediments at three basins (Abu Gharadig, Shushan, and Alamin basins). Bahariya, Abu Roash, and Khoman formations are the three formations that make up the Upper Cretaceous sequence (Issawi et al. 1999). Above the Kharita Formation is the Bahariya Formation (Early Cenomanian) (Albian). It is made up of intertwined sandstones, shales, and limestones.

In the Abu Gharadig Basin, sand volume increases to the south and southeast (Darwish et al. 1994). The Abu Rosh Development, which dominates the marine formation, is classified into seven lithostratigraphic components, ranging from "G" to "A" (Santonian to Upper Cenomanian). The B, D, and F Members of the Abu Gharadig Basin are mostly carbonates, whereas the A, C, E, and G Members are clastic sediments (Bayoumi 1994 and 1996).

According to (Sharaf et al. 1990, Meshref 1990, 1999; EGPC 1992; Schlumberger 1995; Bayoumi 1996; Dolson et al. 2001; Bakry 2005; Ibrahim 2014), the Western Desert features faults directed NE to ENE, EW, and WNW to NW, representing the two main WNW-ESE, ENE-WSW patterns in the basement to a certain extent (Figure 2). Early Mesozoic features include the Umbarka High, Qattara-Sharib Ridge, Sitra Platform, Bahariya High, and the Misawag Graben, Ghazalat, and Abu Gharadig Basins. The Abu Gharadig basin, which has a NE–SW fault pattern, and the Kattaniya high, which has the NW–SE fault trend, are wide-scale structures in the Western Desert (Ibrahim 2014). Most of the folds formed during the late Cretaceous–early Tertiary tectonic event correspond to a general NE–SW pattern (Syrian Arc System) and plunge to the southwest (Said 1962; Kostandi 1963).

3. Methodology

3.1. Data source

The geophysical data were used in the present study in the shape Bouguer gravity anomaly map of scale 1:500,000 updated from GETECH Group PIC (Getech 1992; Green et al. 1992). In addition to data published in articles including Abdelmaksoud (2017), AbuHashish et al. (2020), and Saleh et al., the available subsurface information of 48 deep wells was collected from oil companies (the Egyptian General Petroleum Company EGPC, the Gulf of Suez Petroleum Company GUPCO, and the British Petroleum Company BPC) (2021).

These wells are scattered over the entire region (Figure 1a) and help build a set of gravity anomaly maps for different depositional cycles. These maps (especially the gravity anomaly map of cycle III) and well data were used to construct empirical relationships between gravity and reservoir parameters applied in estimating the reservoir characterisation in the study area.

3.2. Processing and interpretation of gravity data

Many issues arise when interpreting gravitational data, such as isolating anomalies of relevance from the overlapping impacts of other features. Furthermore, the Bouguer map depicts horizontal changes in gravity acceleration; only variations in density cause abnormalities. Vertical density variations have the same impact everywhere; therefore, there are no abnormalities. Furthermore, any region's Bouguer anomaly map is calculated as the sum of gravitational impacts of several lithostratigraphic units, including the sedimentary cover and the foundation complex. The overall gravity impact of an anomalous body was thought throughout this column to be generated by combining the gravity impacts of a vertical prism with a horizontal bottom surface. Some techniques need to be applied to filter the observed gravity data to overcome these problems. In the present study, the gravity stripping technique has been applied to the

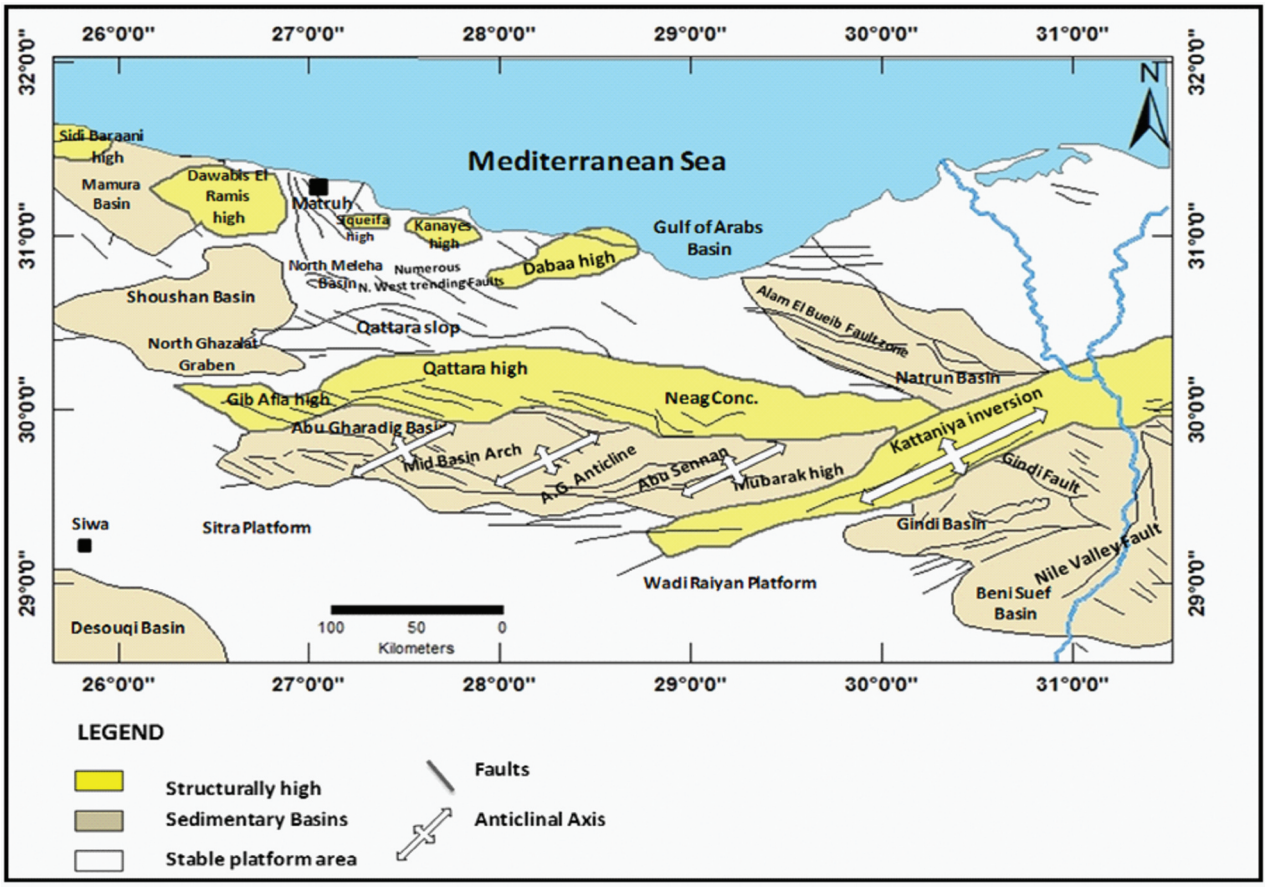

Figure 2. General structure in the Northern Western desert, Egypt, altered after (Bayoumi 1996).

Bouguer gravity anomaly map to separate the gravity effect of each sedimentary cycle recognised in the study area.

Striping gravity technique, the density of interfering objects is known to be sufficiently exact, is regarded as a more accurate physical foundation than any other mathematical approach to gravity field analysis (Nedelkon and Burnev 1962 and Skeels, 1965). The following major steps for applying the stripping technique:

(1) Measurement of the gravity effects of each depositional cycle based on the thickness and density obtained from the well logs of the deep wells in the study area (Table 1).
(2) The calculated gravity values of each depositional cycle were subtracted from the original Bouguer gravity anomaly map (Figure 3) till the basement rocks.

(1) A gravity anomaly map for each deposition cycle is prepared.

The equation used to calculate the gravity effect of each depositional cycle is $\Delta \mathbf{g} = \mathbf{2}\ \boldsymbol{\pi}\ \mathbf{G}\ \boldsymbol{\rho}\ \mathbf{h}$, where Δg represents the gravitational impact of a unit in a gal, G is the international gravitational constant, equal to 6.667×10^{-8} c.g.s unit, ρ is the density contrast between the unit density and the basement rocks density (2.67 g/cm^3), and h is the unit thickness in cm. The gravity effect of the clastic cycles has been determined using density contrast equal to 0.12 g/cm^3 (calculated from the difference between the density of sandstone 2.55 g/cm^3 as obtained from the well logs and the average density of the basement rocks 2.67 g/cm^3). Meanwhile, the gravity effect of the carbonate cycles in the form of limestone was determined using the density contrast of 0.2 g/cm^3 (calculated from the difference between the density of limestone of 2.87 g/cm^3 as obtained from the well logs and the average density of the basement rocks 2.67 g/cm^3).

Applying the stripping technique, six Bouguer gravity anomaly maps were prepared after removing the effect of gravity for each sedimentation cycle (cycle I, II, III, IV, V, the whole sedimentary cover, and the basement rock) as illustrated in Figures 4 and 5.

3.3. Using the gravity data to infer reservoir characterisation

Knowledge of the distribution of porosity, density, permeability, and hydrocarbon saturation in sedimentary rocks are key specifications of the economic evolution of hydrocarbon accumulation (Worden and

Table 1. The drilled wells in the study area and the thickness of each depositional cycle.

Well name	Thickness of cycle 1/ Palaeozoic to lower Jurassic	Thickness of cycle 2/ M -U Jurassic	Thickness of cycle 3/ Lower Cretaceous. To Cenomian	Thickness of cycle 4/m. Eocene	Thickness of cycle 5/Recent
Gib Afia-1	528	846	1176	391	130
Bahrein	1412		1215	412	
N. Ghazalat	533	526	1066	1095	680
Ghourab-1			590	1623	684
Ei Kifar-1	338	73	1705	667	211
Zarif-1x		315	1041	209	798
Ras Qattara-1x	515	527	880	276	379
Ghazalat-1	728	287	1354	414	229
El Kheit-1		336	1703	595	576
Betty-1	820	1257	844	675	379
White R.V. H-1			280	660	
Marzuk-1		882	922	454	653
WD 5–1			1074	2174	1147
Aghar-1x			876	354	1051
Sonomein-1x			1026	657	1271
Sonhur-1x			979	482	1192
Rabat-1	857			792	546
WD 32–1			400	1977	864
Abu Sennan-1			1436	1073	640
Agnes-1	176	525	797	730	360
Miswag-1	52	129	703	934	333
Tiba-1x	214	668	544	961	644
WD 12–1		285	886	1782	616
Mubarak-1			1578	994	210
WD 33–1			419	2489	821
S.W. Mubarak-1		403	1378	1391	404
WD 57–1	385	452	666	988	482
Diyur-1	464		490	176	495
Garif-1		633	700	442	1038
Qattara Rim-1x	748	751	467	283	997
Sharib-1x		289	170	473	887
Ghoroud-1x			847	626	973
WD 7–1				2311	1090
WD 7–2				979	930
WD 8–1			1444	1329	933
Abu Ghar-1				1836	1079
Abu Ghar-3				2132	1104
Khatatba-1	22.1	1505.9			366.6
Abu Roash-1	334.2	801.4	593.9		65.7
Camel Pass W.W.1,2				419.7	44.8
Wadi Natrun-1	232.7	1145.3	1023.8	667	975.6
El Nashfa	183.9		429.4	115.1	
Abyad W. W.,2			258.2	86.6	
Agila					309
Gebel Agila				52	97
Wadi El Raiyan No. 1			425.7	831.7	
Abu Ghar-2	793	1866	1018		
Bahariya A-1X	26.8		509.5	1885	
Karama 3					

Morad 2000). The present study assesses the reservoir characterisation in the North-Western Desert, especially in the Abu Gharadig basin and the surrounding parts. The main source rock is the sandstone of Bahariya and Kharita formations (belonging to Cenomanian and Albian) for the main gas pay, while of Abu Roash Formation (belonging to Cretaceous Turonian to Cenomanian) for the main oil pay (Hanter, 1990). Bahariya, Kharita, and Abu Roash Formation belong to the depositional clastic cycle III. Therefore, the reservoir characterisation calculation procedures were applied to the gravity map of cycle III (Figure 4c). Density and effective porosity information about this cycle was deduced from the available well logs of the deep wells (Table 2). The values of the two parameters were used to establish a linear relationship with the corresponding gravity values. Figure 6a demonstrates the linear correlation between gravity and density values with a correlation coefficient of 0.91. The resulting equation is $\mathbf{\Delta g = -42.932 \rho + 96.434}$, where Δg is the effect gravity value, and ρ is the density value. This equation can be useful for

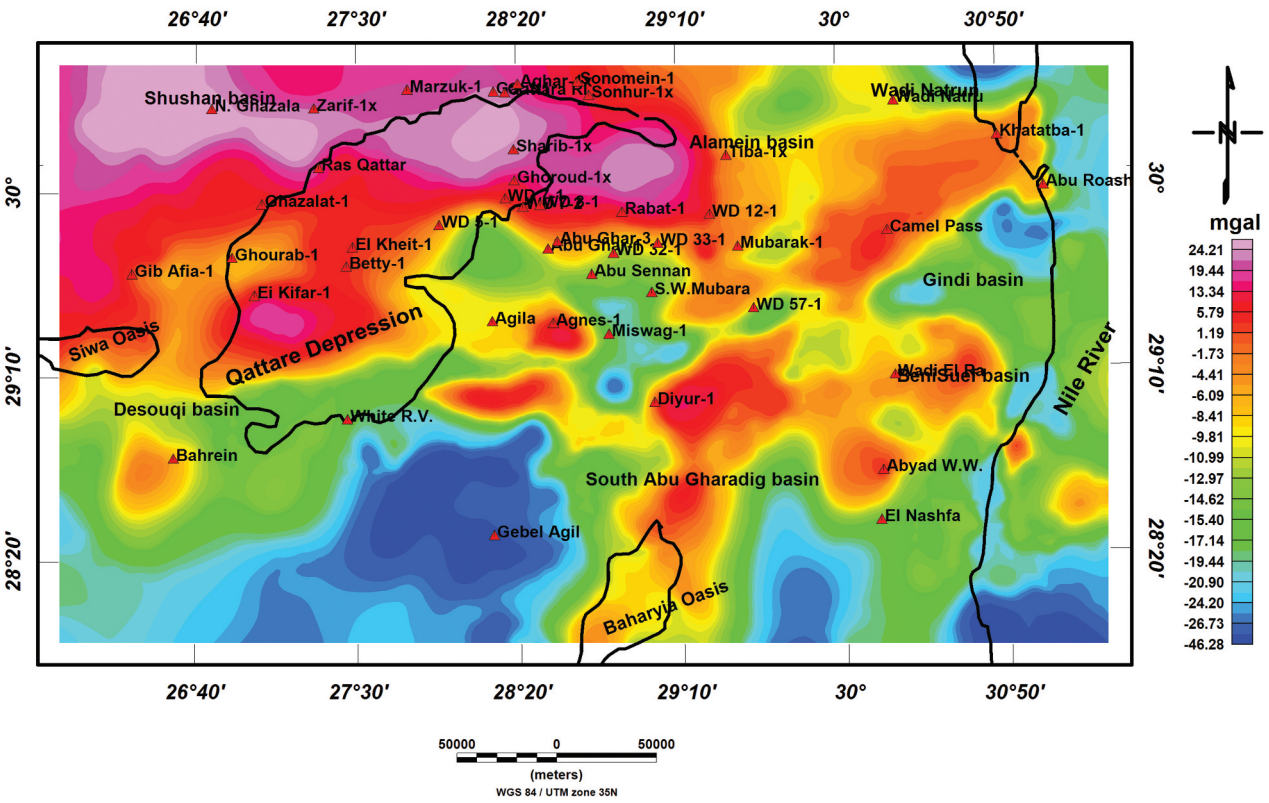

Figure 3. Bouguer anomaly map of the area under study, Western Desert, Egypt (after, E.G.P.C).

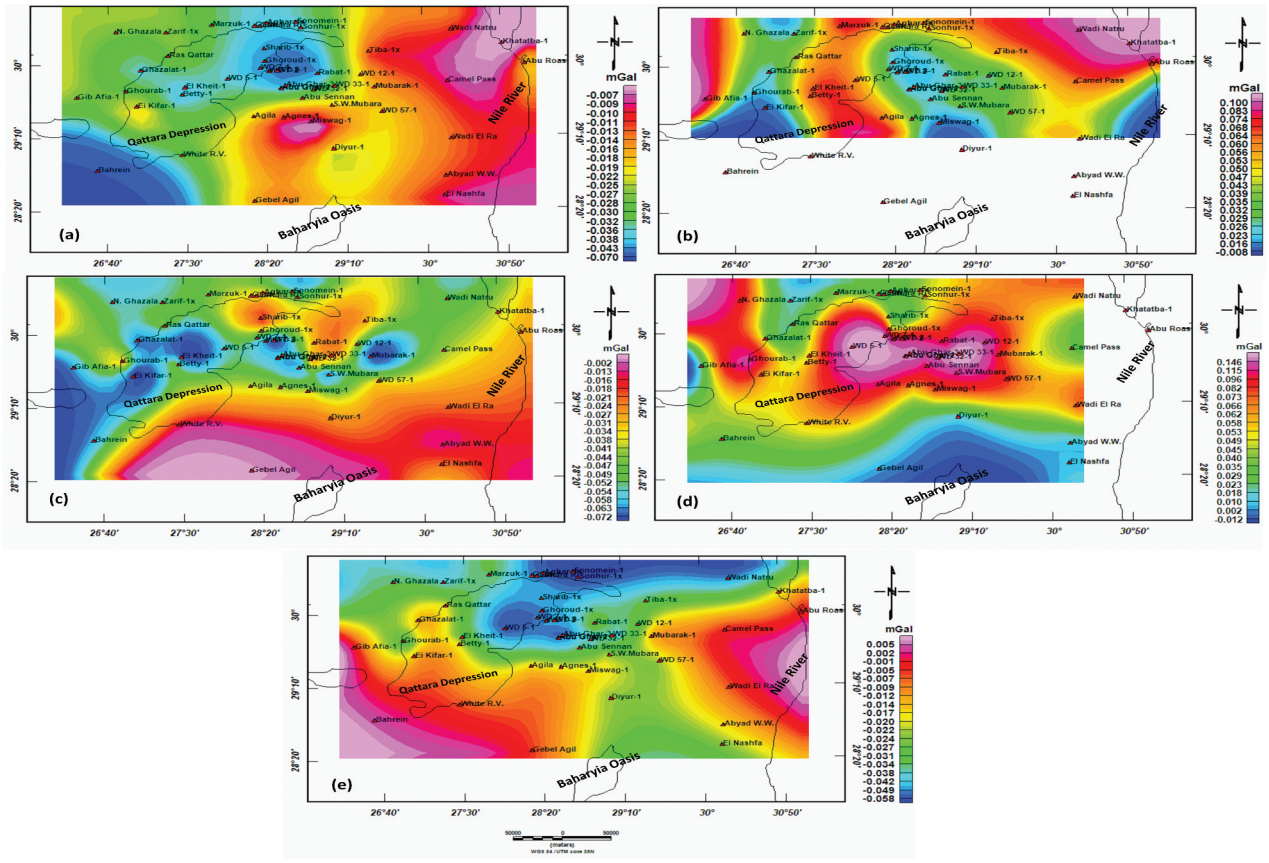

Figure 4. Gravity effect map of different depositional cycles a) cycle I, b) cycle II, c) cycle III, d) cycle IV and e) cycle V.

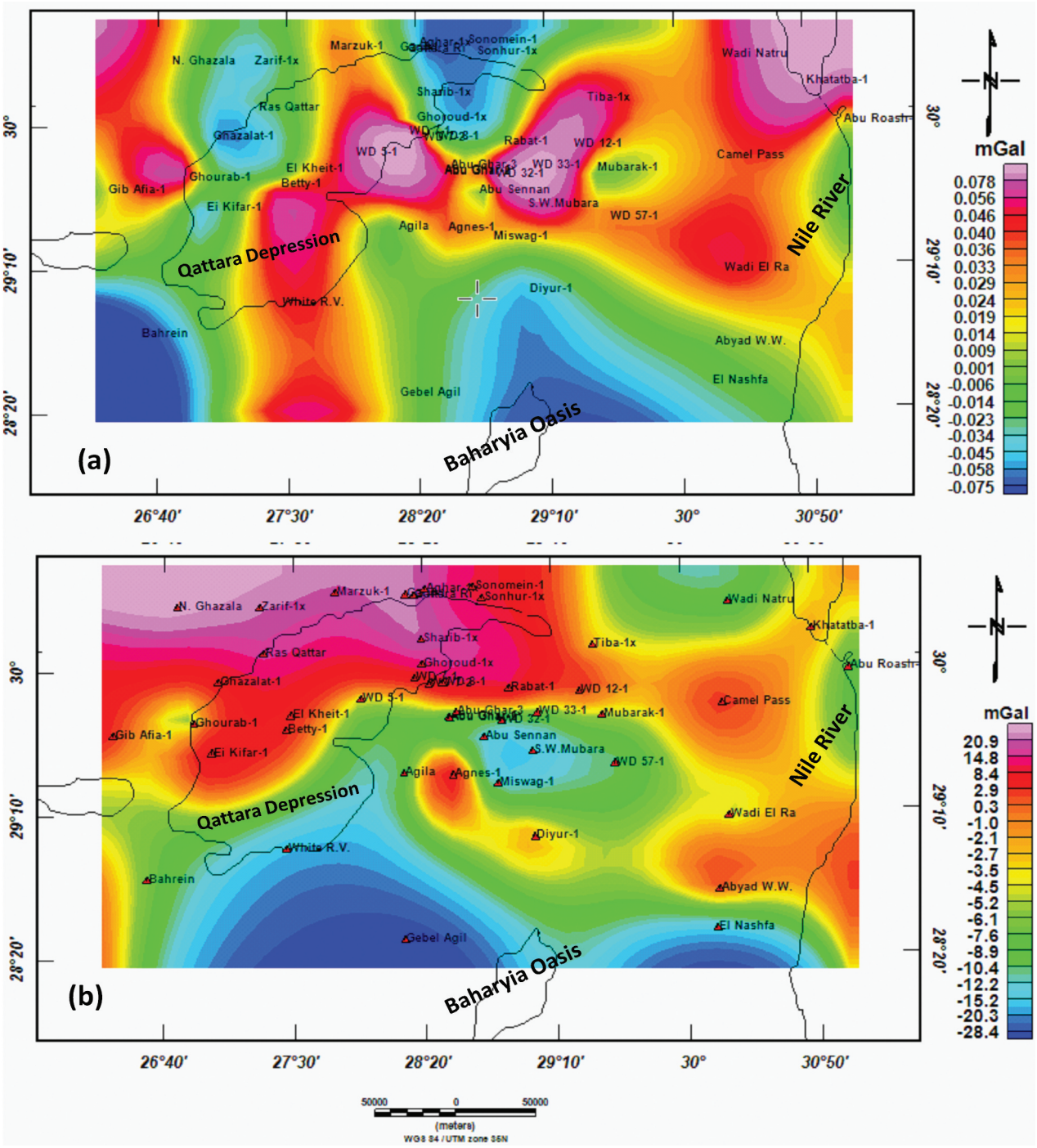

Figure 5. Gravity impact map of a) the whole sedimentary cover b) top basement surface.

determining the density values utilising gravity values at the parts of the study area in which no well logs data are available. Figure 6b,c indicate the linear correlation between gravity values and effective porosity and hydrocarbon saturation with a correlation coefficient of 0.9. The resulting equations are $\Delta g = -0.552\ \Phi_e + 1.4301$ and $\Delta g = -0.2068\ Sh_c + 4.642$, where Φ_e is the effective porosity value, Sh_c is hydrocarbon saturation. Applying these equations, the values of effective porosity and hydrocarbon saturation were calculated through gravity values in the parts of the study area where no well logs data are available.

4. Results and discussion

The qualitative interpretation of the Bouguer anomaly map (Figure 3) reveals the presence of many closed anomalies of various shapes (oval, elongated), trends, and amplitudes. The features of the underlying rocks and the overlying sedimentary cover are referred to as anomalies. With rising northward distance, the magnitude of most gravity anomalies ranges from −45 to +30 mgal. The northern part has positive gravity anomaly values starting from 3 to 30 mgal with a remarkable northward increase. The south part,

Table 2. Petrophysical parameters as deduced from the used lithological logs of the deep wells in the study area, and its corresponding gravity values obtained from the gravity effect of cycle III.

Well name	Density (g/c^3)	Effective porosity (%)	Hydrocarbon saturation (%)	Gravity effect value of cycle 3
1	2.5	19	70	−10.15422836
2	2.4	14	56.92	−6.450535363
3	2.34	10	45	−3.987151052
4	2.35	10	40	−3.611820497
GPT1	2.5	21	80	−10.52418157
Baharyaia A1x	2.5			−10.08066186
Karama 3	2.45	22	61.5	−8.817609464
Karama 4	2.45	20	65	−9.450965446
Karama 13	2.45	20	70	−10.26532685
Karama 14	2.45	19	65	−9.432029437

which also started at latitude southward, has negative gravity values ranging between −5 and −45 mgal. These two main parts constitute two major tectonic units. The northern one, which may be represented down faulted blocks of old sediments, started from Cambrian to Quaternary, Said (1962). These sediments in some locations are saturated by oil and/or gas, and in others are saturated by saline water. Therefore, these sediments are denser than the surrounding rocks resulting in a positive gravity anomaly. Meanwhile, El-Gamili (1968) indicates that the increase in the gravitational field may be due to a northward decrease in crustal thickness. Inversely, the sediments are mostly clastic, starting in age from Palaeozoic to Recent in the southern part. These sediments' pours and permeable parts are saturated by fresh groundwater (Nubian aquifer). Therefore, they have less density than the outer or the country rock and give a negative gravity value. The major closed negative anomalies in the southern parts of the area are mainly at Abu Ghradig and ElGinidi basin. All these are considered basins of oval shape. The other minor closed negative anomalies are predominating at Abu Ghradig. These anomalies represent local basins inside the major area. The major linear anomalies in all areas have NE-SW and E-W trends.

By applying the gravity stripping technique, seven gravity anomaly maps were prepared for the depositional cycles I, II, III, IV, V, the whole sedimentary cover, and the top of basement rocks after removing the gravity effects of the sedimentary cover (Figures 4 and 5). These maps reveal the distribution of the gravity effect of each depositional cycle and the top of basement rocks. The gravity anomaly map of the depositional cycle I (Figure 4a), which included the

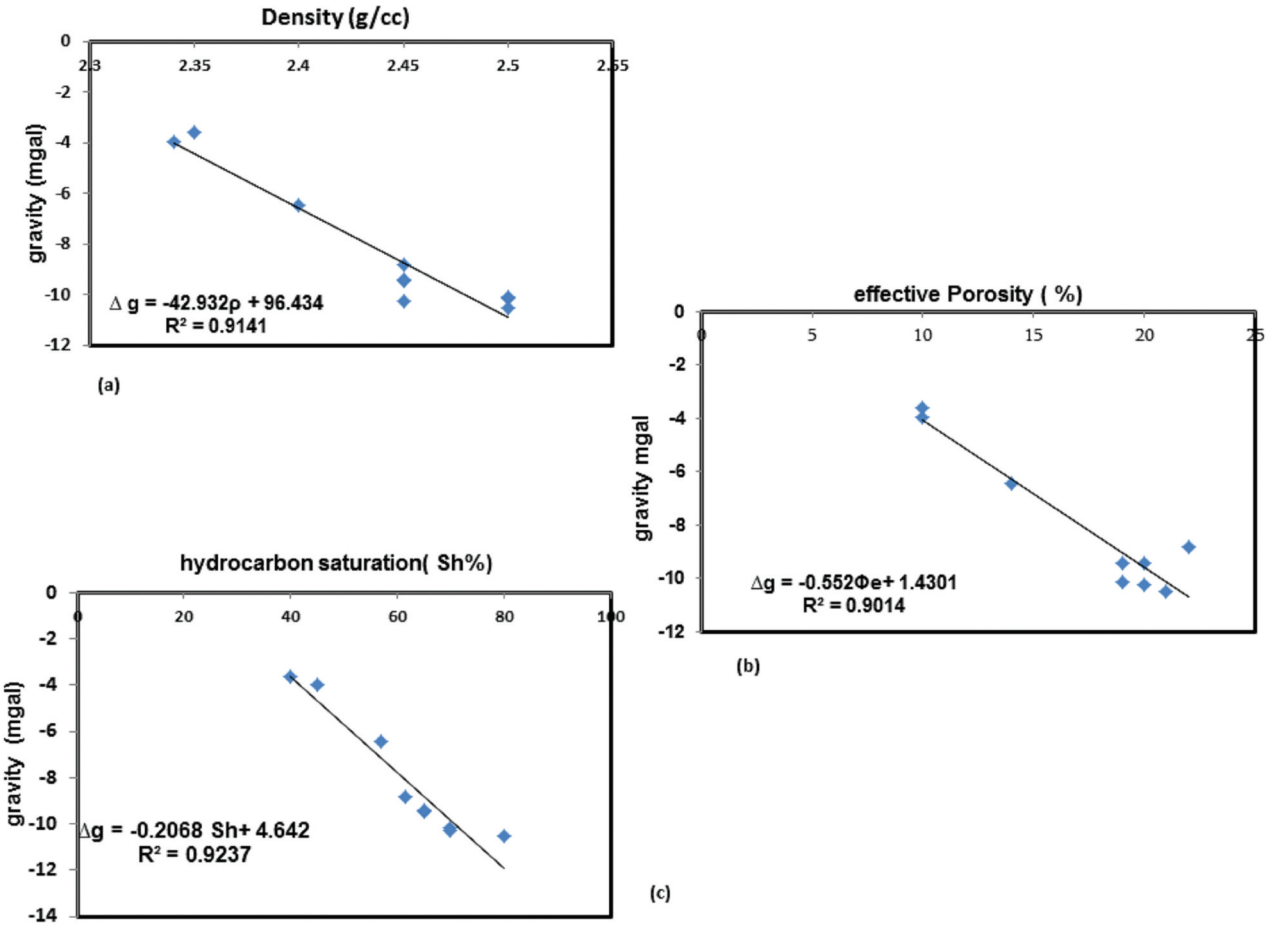

Figure 6. Relations between gravity values and petrophysics parameters such as a) density b) effective porosity and c) hydrocarbon saturation.

oldest sedimentary rocks, shows that the measured gravity values range from – 0.07 to −0.007 mgal. The low and high gravity values are recorded in the western and eastern parts of the study area, respectively. The gravity variation indicates lateral variation in the thickness of sedimentary cycle I. (Figure 4b) shows the gravity anomaly map of depositional cycle II, which constitutes Middle and Upper Jurassic formations. The calculated gravity values vary from – 0.008 to 0.1 mgal. The increase in the gravity values is accompanied by an increase in the number of carbonate rocks (high-density rocks) compared to clastics in sedimentary cycle II. Figure 4c represents the gravity anomaly map of depositional cycle III, which constitutes the Lower Cretaceous up to the Upper Cretaceous Early Cenomanian sediments that constitute the Western Desert's primary hydrocarbon sources. The gravity values calculated range is from −0.07 to −0.002 mgal.

Several circle low anomalies (−0.07 mgal) can be seen in the research area's core areas, extending in the N-S direction along the main axis of the Abu Gharadig basin. The gravity values increase towards the south. Most anomalies mainly have trends in E-W, N-S, and NW-SE directions. The low gravity values indicating the thickness of the sediments in these regions increased (1400 m), noticeably in (Figure 7), where the isopach map of depositional cycle III. Figure 4(d,e) show the gravity anomaly for depositional cycle IV and cycle V, respectively. These maps show that the calculated gravity values increase as depositional cycle IV (Figure 4d) due to the high density of carbonate rocks. The gravity value reduces in (Figure 4e) where the clastic rocks. Meanwhile, a summation of the gravity values of all depositional cycles was produced to depict the gravity anomaly map of the whole sedimentary (Figure 5a). Conversely, the basement surface's gravity effect without the sedimentary cover's influence can be seen in (Figure 5b). On this map, the magnitude of the anomalies varies from −28 mgal in the southern parts to 21 mgal in the northwestern part of the study area. The general trends of the elongated and linear anomalies are mainly in the E-W, NE-SW, and NW-SE directions. The trend of gravity faults tracked by all stripped gravity maps in the study area is illustrated in (Figure 8). This map indicates the dominant subsurface structural trends from Precambrian to recent according to all depositional cycles: the E-W, the WNW-ESE, the ENE-WSW, the NE-SW, the NW-SE, and the N-S trends.

In contrast, three empirical relationships were obtained between the petrophysical parameters (density, effective porosity, and hydrocarbon saturation), and the calculated gravity value of cycle III (the main hydrocarbon reservoirs) in the study area in which well logging and borehole data were available. Of these relations, the mentioned petrophysical parameters were calculated for the parts of the study area in which no wells or excavations occurred.

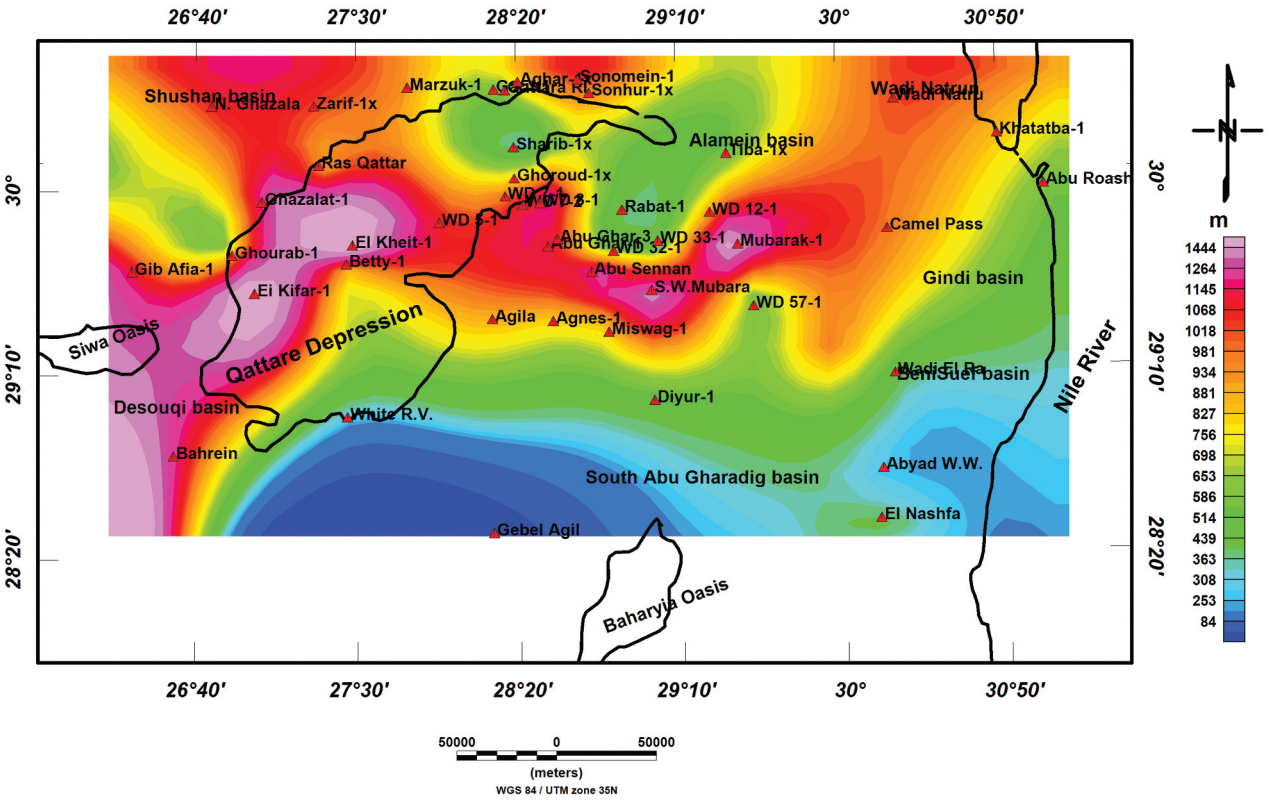

Figure 7. Example of isopach map for depositional cycle III.

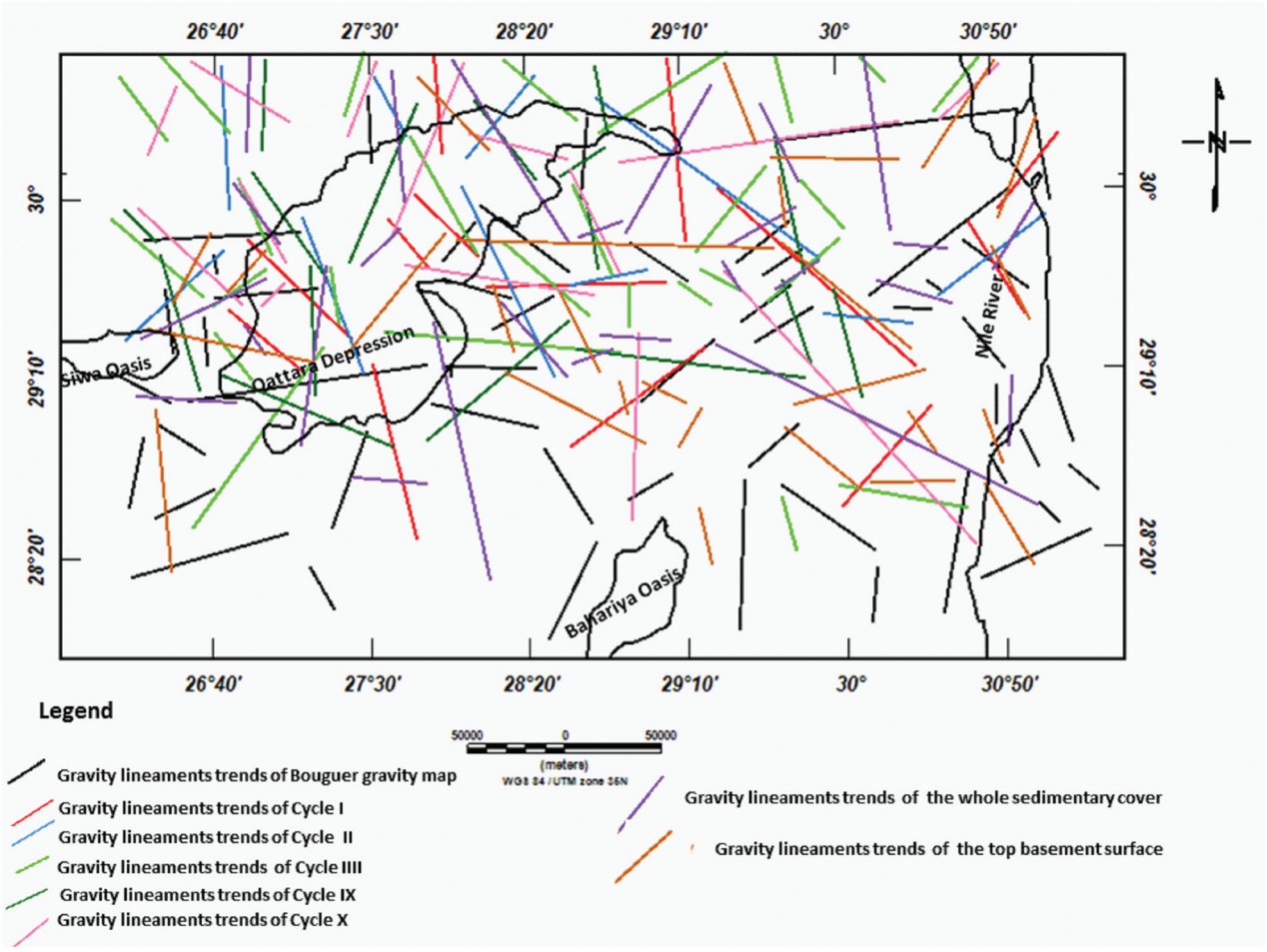

Figure 8. Gravity lineaments trends as interpreted from bouguer anomaly map and its derivatives from stripping technique (gravity effect maps of different depositional cycles).

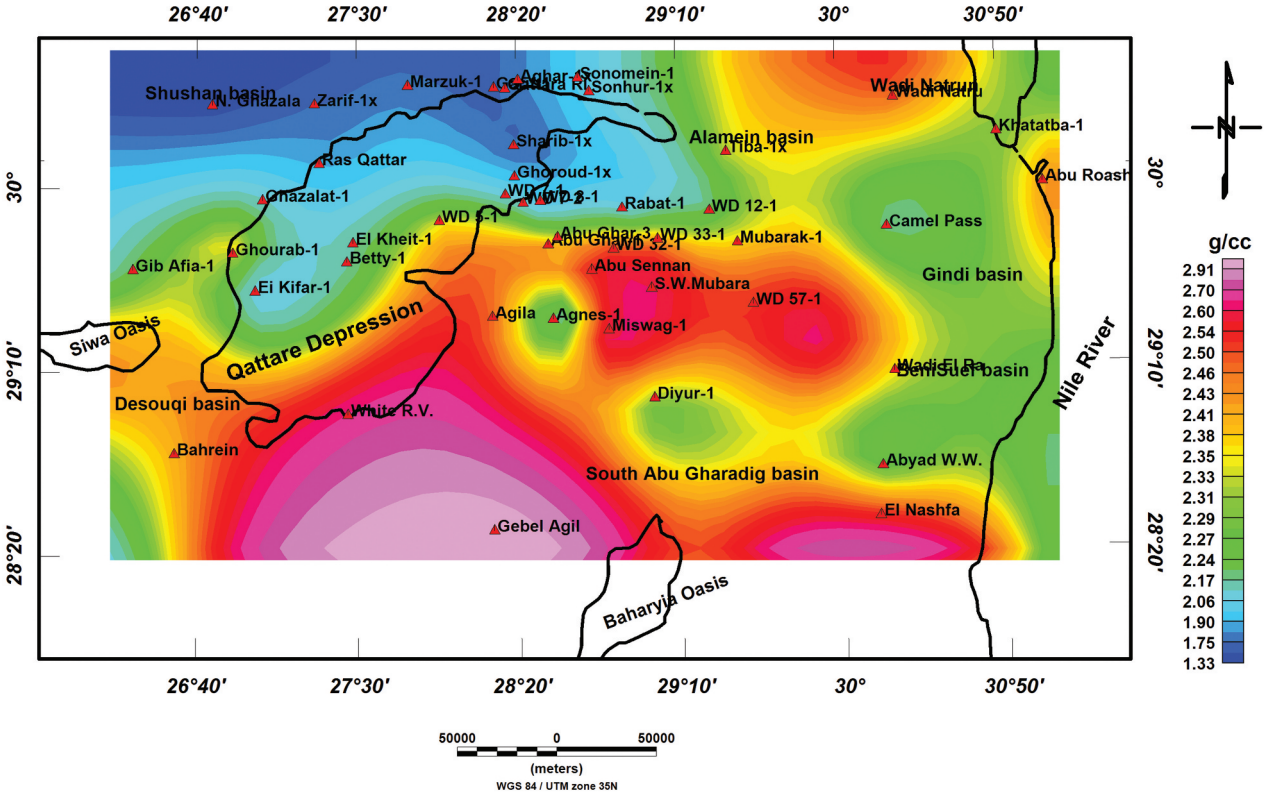

Figure 9. Predicted density map of the study area.

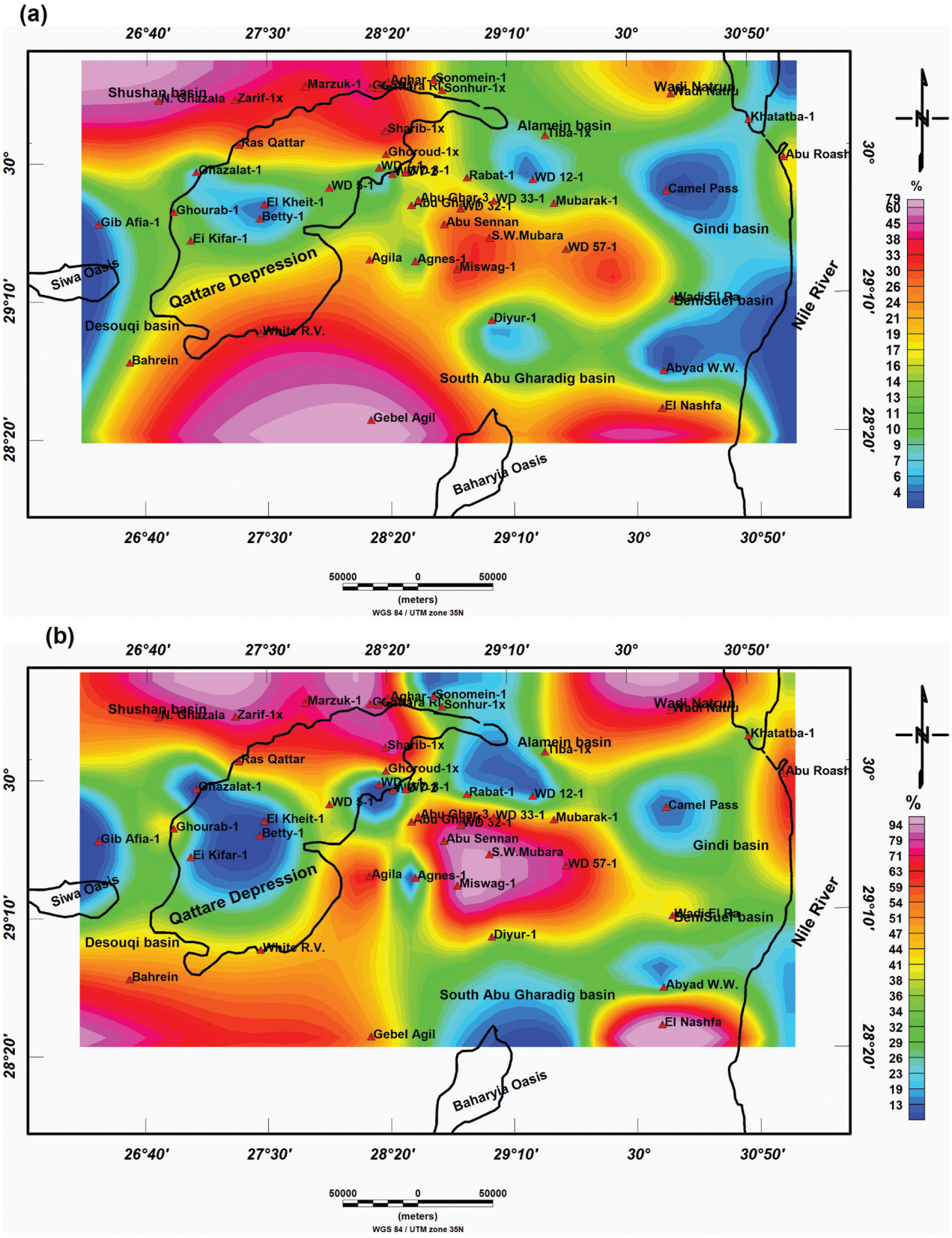

Figure 10. A) Predicted effective porosity map b) Predicted hydrocarbon saturation map of the study area.

Accordingly, contour maps (Figures 9 and 10a,b) were prepared for the density, effective porosity, and hydrocarbon saturation of the sedimentary cycle III (the main hydrocarbon reservoirs in the study area). Remarkably, from these maps,the density of the reservoir changed from 1.3 g/cm^3 to 2 g/ cm^3 at the Alamein basin, from 2.2 g/cm^3 to 2.33 g/ cm^3 at Ginidi and Beni Suef basin, from 2.3 to 2.45 g/cm^3 at Natrun basin and increased to more than 2.75 g/cm^3 in the southern parts at Gabal Agil. Meanwhile, the density value ranges from 2 to 2.7 g/ cm^3 in the Abu Gharadig basin. The calculated

effective porosity varies from 3% to 10% at Ginidi and Beni Suef basin in the western Nile valley, 13% to 30% at Abu Gharadig basin, and 30% to 60% at the Shushan basin in the north. The calculated hydrocarbon saturation ranges from 40% in the Gindi basin and 50% to 90% in the north of Abu Gharadig, Desouqi, Natrun, and Shushan basin, while decreasing to 20% in the south Abu Gharadig basin.

Generally, the results obtained from the predictive maps of sufficient hydrocarbon saturation and porosity are consistent with some previous works results; for example, Saleh et al. (2021) concluded that the effective porosity in the Karama oil field varies from 18.3% to 33.3%, and the hydrocarbon saturation was more than 61.5% in some zones. Meanwhile, the present study displays that the effective predictive porosity varies from 18% to 28%, while the predictive hydrocarbon saturation reaches 55%, especially in the western zones (Figure 10).

5. Conclusions

(1) The main subsurface structural trends deduced from the interpretation of the gravity maps of the five sedimentary cycles (I, II, III, IV, and V) defined in the study area are: the E-W, the WNW-ESE, the ENE-WSW, the NE-SW, the NW-SE, and the N-S trends.
(2) Respectable empirical relationships between gravity and the petrophysical parameters (density, effective porosity, and hydrocarbon saturation) were established. Accordingly, some of the reservoir characterisation of cycle III, the major hydrocarbon reservoir in the study area, was calculated.
(3) Bouguer gravity data gave a preliminary prediction of reservoir characterisation of the study area.
(4) Three new density, effective porosity, and hydrocarbon saturation maps were constructed of the Northern Western Desert.
(5) These new maps were accessed to predict the petrophysics parameters such as density, effective porosity, and hydrocarbon saturation at localities where no boreholes exist.
(6) The calculated density values range from 1.5 g/cm^3 to 2.9 g/cm^3 in the Northern Western Desert.
(7) The calculated density value varies from 2.3 g/cm^3 to 2.7 g/cm^3; meanwhile, the estimated effective porosity ranges from 13% to 30%. However, the hydrocarbon saturation ranges from 50% to 90%. These calculated values display a decent concordance with the values obtained from well logs of wells drilled in the Abu Gharadig basin (Mubarak −1, Abu Sennanm, and Ghar 1, 2,3).
(8) The calculated reservoir characterisation indicates that any future exploration of hydrocarbons in the study area must prioritise Natrun and Shoushan basins in the northern parts and the Desouqi basin in the southwestern part. The expected hydrocarbon saturation in these parts ranges from 70% to 90%.

Disclosure statement

No potential conflict of interest was reported by the author(s).

References

Abdelmaksoud A, (2017): Integrated geological modeling of the upper Bahariya reservoir in Abu Gharadig oil and gas field, north western desert, Egypt. M.Sc, Thesis. Faculty of Science, Assiut University: Egypt 148

Aboelhassan N, Tarabees E, Alaa M. 2017. Reservoir evaluation of Bahariya formation in tut oil field, North Western Desert, Egypt. International Journal of GEOMATE. 12(29):195–203.

Abu Shady AN, El-Shishtawy AM, Abdel Hameed AT (2010): Reservoir characterization of the upper cretaceous Bahariya formation, Khalda ridge, north Western Desert, Egypt. Proceedings of the 6th International Symposium on Geophysics, Tanta, Egypt, p. 34–46.

Abu-Hashish M,F, Said A. 2016. Volumetric assessment through 3D geostatic model for Abu Roash "G" reservoir in Amana field-east Abu Gharadig basin-Western Desert-Egypt. J Geol Geophys. 5: 2. 10.4172/2381-8719.10002 42.

Abuseda H, Weller A, Sattler CD, Debschütz W. 2016. Petrographical and petrophysical investigations of upper cretaceous sandstones of the south west Sennan field, Western Desert, Egypt. Arabian Journal of Geosciences. 9(3):1–18. doi:10.1007/s12517-015-2156-1.

Bakry G (2005): Facies modelling and hydrocarbon trapping mechanism of some selected upper cretaceous—tertiary reservoirs Badr El-Din and Sitra concessions, Western Desert, Egypt. PhD thesis. Faculty of Science, Al-Azhar University, Egypt, pp 16, 19

Bayoumi T, (1994): Syn sedimentary tectonics and distribution of Turonian sandstone reservoirs, Abu Gharadig basin, Egypt. Roc. EGPC 12th petrol. Expl. Prod. Conf. Cairo, Vol. I, pp. 351–367

Bayoumi T (1996): The influence of interaction of depositional environment and syn-sedimentary tectonics on the development of some late cretaceous source rocks, Abu Gharadig Basin, Western Desert (Egypt)

Bekhiet MH, El-sawy EK, El-fouly HE, Fathy M, Abd El-Motaal E, Khalil RM. 2011. Subsurface structural and petrophysical study on Karama field, east bahariya concession, Western Desert, Egypt., Al-Azhar Bull. Sci. 22(2):61–79.

Darwish M, Abukhadra AM, Abdelhamid ML, Hamed A, (1994): Sedimentology, environmental conditions and hydrocarbon habitat of the Bahariya formation, central Abu Gharadig basin, Western Desert, Egypt. Proc. EGPC 12th Petrol. Expl. prod. Conf., Cairo, Vol. I, pp. 429–449

Dolson J,C, Shann M,V, Matbouly S, Harwood C, Rashed R, Hammouda H. 2001. The petroleum potential of Egypt. In: Threet M. W., Morgan, W. A., editors. Petroleum provinces of the twenty-first century, AAPG memoir 74. p. 453–482.

EGPC. 1992. In Western Desert, oil and gas fields, a comprehensive overview Paper presented at the 11th Petroleum Exploration and Production Conference, Egyptian General Petroleum Corporation, Cairo, Egypt. p. 1–431.

El- Gamili MM, (1968): Regional geophysical investigation, Northern Western Desert, Egypt: ph.D. Thesis, Fac. Sci., Assiut Univ., Assiut, Egypt, 276 p.

El-Hossainy MM (2008): Reservoir characterization and sedimentology of some Cretaceous reservoirs in Abu Gharadig basin, Western Desert, Egypt. M.Sc. Thesis, Faculty of Science, Assiut University, Egypt. 199 p.

El-Shaarawy OA, Zaafan S, Rashed R, Lelek J, El Leboudy M, Hadidy A (1994): Jurassic hydrocarbon potentiality in the Abu Gharadig basin, North Western Desert of Egypt. In: 12th EGPC exploration and production conference Cairo, vol 2, pp 234–247

Gadallah M, Samir A, Ghoneimi A, Nabih M (2004): Seismic and well logging analysis of Bahariya formation in Aghar oil field, North Western Desert, Egypt. Proceedings of the 10th Formation Evaluation Symposium of Japan, p. 1–14.

Gadallah M, Samir A, Nabih M. 2010. Integrated reservoir characterization studies of Bahariya formation in the Meleiha-NE oil field, North Western Desert, Egypt. Earth Sciences. 21(1):111–136.

Getech. (1992): The African magnetic and gravity mapping project—commercial report (unpublished)

Green CM, Barritt SD, Fairhead JD, Misener DJ (1992): The African magnetic and gravity mapping project. Extended abstract, EAEG 54th Meeting and Technical Exhibition, Paris

Ibrahim H, (2014): Structural style and hydrocarbon trapping of East Bahariya, using 3d seismic data application and interpretation; Western Desert, Egypt. MSc thesis, Faculty of science, Ain Shams University, Egypt, pp 48–49

Issawi B, El-Hennawy M, Francis M, Mazhar A. 1999. Geological interpretation of the main geomorphic units in Egypt. Phanerozoic Geology of Egypt, Geodynamic Approach, Special Publication. 76.

Keeley ML. 1989. The Paleozoic history of the Western Desert of Egypt. Basin Research. 2(1):35–48. doi:10.1111/j.1365-2117.1989.tb00025.x.

Kostandi AB, (1963): Eocene facies maps and tectonic interpretation in the Western Desert, Egypt. Revue de l' Institute Francais

Meshref W, Rafai E, Sadek H, Abdel-Baki S, El-Sirafe A, El-Kattan E, El-Meliegy M, El-Sheikh M. 1980. Structural geophysical interpretation of basement rocks of the North Western Desert of Egypt. Annual Meeting of Geological Survey of Egypt. 10:923–937.

Mohamed AK, Ghazala HH, Mohamed L. 2016a. Integration between well logging and seismic reflection techniques for structural analysis and reservoir characterizations, Abu El Gharadig basin, Egypt. NRIAG Journal of Astronomy and Geophysics. 5(2):362–379. doi:10.1016/j.nrjag.2016.07.003.

Nedelkon I,P, Burnev P,H. 1962. Determination of gravitational field in depth. Geophysical Prospecting. 10 (1):1–18. doi:10.1111/j.1365-2478.1962.tb01995.x.

Said R. 1962. The geology of Egypt. Amsterdam-New York: Elsevier; p. 377.

Saleh A,H, Farag A,E, Eysa E,A. 2021. Reservoir quality of Abu Roash (G) member in Karama oil field, east Bahariya concession, North Western Desert, Egypt. Arabian Journal of Geosciences. 14(3):169. doi:10.1007/s12517-020-06349-9.

Schlumberger (1995): Well evaluation conference, Egypt. schlumberger technical editing services, Chester, p. 356.

Sestini G. 1995. Regional petroleum geology of the world part II: Africa, America, Australia and Antarctica. Gebrüder Bornträger Verlagsbuchhandlung, Stuttgart, v. Beiträge Zür Regionalen Geologie der Erde. 22: 66–87. Band.

Sharaf M, El-Awady M, Zahra H. 1990. Gravity and Landsat lineaments in northern Egypt and their significance. Delta Jour Sci Bull. 14: 1–8. Tanta, Egypt.

Worden RH, Morad S. 2000. Quartz cementation in oil field sandstones: a review of the key controversies. Int Ass Sediment Spec Publs. 29:1–20.